Progress In Electromagnetics Research M, Vol. 110, 83–96, 2022

A Circular Triangle Fractal Antenna for High Gain UWB Communications with Band Rejection Capability

Chellappa Muthu Ramya* **and Rajasekar Boopathi Rani**

Abstract—This paper proposes the design and implementation of a circular triangle fractal antenna for portable ultra-wideband (UWB) communication applications with band rejection at WLAN band. The presented antenna is made with iterative generation of circular triangle shaped elements arranged in a circular fashion with self-similarity and periodicity property with coplanar waveguide feed. The overall dimensions of the antenna are $28 \times 27 \times 1.6\,\text{mm}^3$. The fractal resonating plane and ground plane dimensions of the proposed antenna are optimized to obtain a resonance bandwidth of 2.39–12.28 GHz which corresponds to the fractional bandwidth of 134.8% with notch band from 5.45 to 6.27 GHz to mitigate the problem of interference from WLAN. The peak gain detected is 11.16 dBi. The proposed prototype was fabricated on a 1.6 mm thick FR4 material with the relative permittivity of 4.4, and the sample was tested. The experimental results are in close agreement with the simulated ones. The time domain analysis indicates that the proposed antenna is not dispersive. The antenna radiates in a virtually omnidirectional pattern. Due to these merits, this proposed antenna can be used in UWB applications.

1. INTRODUCTION

An extensive research interest has arisen since February 2002, after the Federal Communications Commission (FCC) approved a licence for ultra-wideband (UWB) communication system. It says that the UWB can be utilized for data communications and for tracking and security applications. FCC allocated the band of operation from 3.1 GHz to 10.6 GHz for UWB signals [1]. Thus, the UWB technology has advanced rapidly as it permits short range and ultra-high-speed communications according to the Shannon-Hartley theorem. The UWB system consumes a very low power by means of dividing the power of the signal across the large spectral bandwidth [2].

Within the UWB radio spectrum from 3.1 to 10.6 GHz, some conventional systems exist such as IEEE 802.11a, WiMAX. It is necessary for UWB antenna to reject the frequencies used by other conventional narrow band systems overlapping with UWB range to avoid the interference between them. To address this problem, several techniques have been researched to obtain band-stop characteristics such as incorporating fractal structures [3], cutting slots of different shapes [4], parasitic stubs [5], control strips [6], metamaterial [7], and Electromagnetic Band Gap (EBG) structures [8]. However, many of the techniques have complex structures which leads to high fabrication cost, bulky structure, and being difficult to fit in a microwave integrated circuit. These techniques result in complicated design and are also difficult to implement. The simplest way is the use of slots on radiating element or ground plane.

Fractal characterises rough or broken fragments. The term fractal coined by Mandelbrot in the year 1977 [9]. Fractal is a structure that carries self-similarity and space-filling properties. By utilizing fractals in an antenna, the compactness, wide and multiband characteristics can be achieved [10–13].

Received 6 November 2021, Accepted 26 April 2022, Scheduled 3 May 2022

* Corresponding author: Chellappa Muthu Ramya (ramyacpct@gmail.com).
The authors are with the Department of Electronics and Communication Engineering, National Institute of Technology Puducherry, Karaikal 609 609, India.

Several UWB antennas using the fractal techniques were introduced in the past two decades [14]. A circular Sierpinski carpet fractal UWB antenna has been presented [15] with a meandered slot in the fractal patch to create a notch band. A hexagonal Sierpinski carpet fractal shape UWB antenna has been proposed [16] with band rejection using a Y-shaped slot. A circular apollonian fractal UWB antenna has been reported in which a notch band was created by a couple of L-shaped slots [17]. A modified Sierpinski square fractal UWB antenna has been proposed with a ∩-slot used for band rejection [18]. A modified circular split ring shaped fractal antenna has been proposed in which a sectorial-circular ring is used to produce a band rejection [19].

A wheel-shaped modified fractal antenna for UWB applications has been presented in which miniaturization was achieved by the monopole made of fractured concentric circles with smaller square patches [20]. A decagonal Sierpinski UWB fractal antenna has been presented in which the size reduction was realized by using a square fractal slot on the patch [21]. Based on these fractal concepts, small UWB antennas have been constructed. These designs are not able to produce relatively high gain within compact size.

In this paper, a circular triangle fractal antenna for high gain UWB applications with notch band at WLAN frequency band is proposed. An impedance bandwidth of 9.89 GHz (2.39–12.28 GHz) is covered by the antenna for UWB system. A U-shaped slot is etched at the CPW feed line, which creates a desired peak at notch band from 5.45 to 6.27 GHz without changing the patch size. The paper is organized as follows. Section 2 presents the design procedure of the antenna geometry. The simulated and experimental results along with the parametric study are discussed in Section 3. Finally, the work is concluded in Section 4.

2. ANTENNA GEOMETRY DESIGN

The dimension of the initial structure is calculated from the basic design equations given in [22]. The mathematical expression for resonance frequency 'f_r' of circular patch antenna is given as,

$$f_r = \frac{X_{nm} C}{2\pi a_e \sqrt{\varepsilon_r}} \tag{1}$$

where the value of 'X_{nm}' = 1.8412 for TM_{11} mode. 'C' is the free space light velocity, 'ε_r' the dielectric constant of the substrate, and 'a_e' the effective radius of circular patch which is given as

$$a_e = a\sqrt{\left[1 + \frac{2h}{\pi a_e \varepsilon_r}\left(\ln\frac{\pi a_e}{2h} + 1.7726\right)\right]} \tag{2}$$

where the circular patch physical radius is denoted as 'a', and the substrate thickness is represented as 'h'. By using the standard Equations (1)–(2), a circular patch of radius 13 mm was designed for the lower resonant frequency of the UWB.

It is the fact that the current of the antenna will be particularly distributed along the outer edge of the patch. The surface current density is less at the center of the patch. Hence, removing the center portion of patch will not affect the current distribution. However, the current path will be increased. In this proposed antenna, the current path length has been increased by introducing circular triangle fractal elements. This results in the reduction in the lower resonance frequency which leads to miniaturization.

The fractal construction starts with eight circular patches of diameter 8 mm overlapped with each other which is shown in Figure 1. The intersection portion is removed and arrives at the fractal initiator which is shown in Figure 2 as Antenna 0. This shape can be thought of as eight circular triangles arranged in a circular fashion. Then, a reduced size initiator is added in every consecutive iteration. The fractal structure is shown in Figure 2 as Antenna 2 to Antenna 6. The fractal size reduction factor (δ) followed here is 0.7, which is given in Eqs. (3)–(4).

$$\delta = \frac{a_{n+1}}{a_n} \tag{3}$$

$$\delta = \frac{r_{n+1}}{r_n} \tag{4}$$

where a_{n+1} is the area of $(n+1)^{\text{th}}$ iterative circular triangle, and a_n is the area of the n^{th} iterative circular triangle. r_{n+1} is the radius of upper arc of the $(n+1)^{\text{th}}$ iterative circular triangle, and r_n is

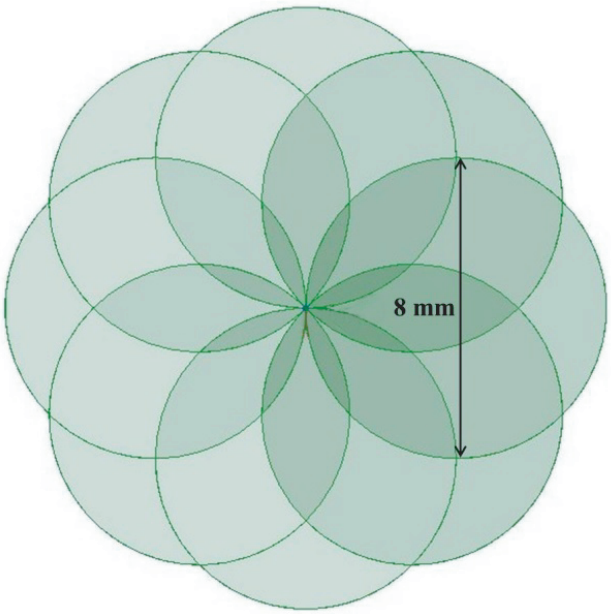

Figure 1. Basic circles.

the radius of upper arc of n^{th} iterative circular triangle from the center of the fractal structure. The stepped-feed, L-shaped defected ground structure and tapered ground were used to further enhance the bandwidth and made the antenna to resonate at the desired frequency band. A U-shaped slot was incorporated on the feed line to achieve band rejection characteristics at WLAN band.

The evolution process of the proposed fractal antenna is shown in Figure 2 from Basic Shape to Antenna 6. The length of U-shaped slot formed on the feed line is closer to the half of the guide wavelength corresponding to the center frequency of the rejection band that is 5.5 GHz. The rejection band frequency can be tuned by adjusting the length and width of the slot. The total length of the slot can be estimated from Eq. (5),

$$l_{slot} = \frac{c}{2f_{notch}\sqrt{\varepsilon_{eff}}} \tag{5}$$

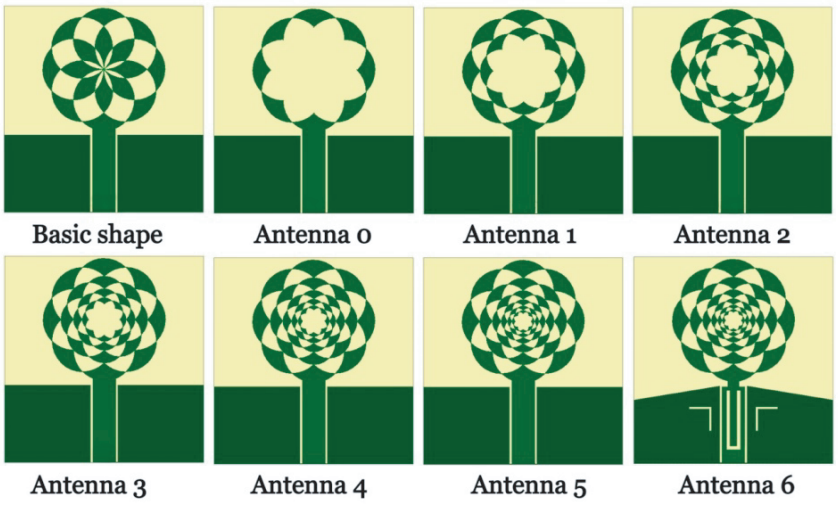

Figure 2. The evolution process of the proposed antenna.

where 'l_{slot}' is the total length of the slot, 'c' the free space light velocity, 'f_{notch}' the center frequency for the notch band, and 'ε_{eff}' the effective dielectric constant of the substrate. To achieve 50 Ω impedance, the width of the CPW feed and the gap between the conductor and ground were calculated by using the standard equations. The proposed circular triangle fractal antenna structure labeled with optimized dimensional parameters is shown in Figure 3. The optimized antenna dimensional parameters are listed in Table 1.

Table 1. Optimized antenna dimensional parameters seen in Figure 3.

Parameter	Description	Dimension (mm)	Parameter	Description	Dimension (mm)
l_{sub}	length of the substrate	28	l_{g1}	inner length of the ground	10.5
w_{sub}	width of the substrate	27	l_{g2}	outer length of the ground	8.6
R_1	radius of circles	8	l_l	length of the L-slot	3.3
h	height of the substrate	1.6	w_l	width of the L-slot	3
g	gap distance between feed and ground	0.3	l_u	length of the U-slot	8.035
l_{f1}	length of the feed	10.4	w_u	width of the U-slot	1.87
l_{f2}	length of the step feed	0.77	t	gap distance between patch and ground	0.6
w_{f1}	width of the feed	3.1	lw_l	Line width of the L-slot	0.3
w_{f2}	width of the step feed	1.5	lw_u	Line width of the U-slot	0.47

3. RESULTS AND DISCUSSIONS

3.1. Effect of Iteration

Figure 4 shows the return loss characteristics of the antenna with respect to its iteration stages of fractal structure between the frequencies of 1.0 and 14.0 GHz. It is clear that if the iteration increases, the impedance matching improves, and the antenna produces wideband. It is observed that iteration 5 which is mentioned as Antenna 5 in Figure 2 gives impedance bandwidth at the desired frequency range. The Antenna 6 in Figure 2, in which the U-shaped slot incorporated on the feed, produces a notch at WLAN frequency range.

3.2. Effect of Tapered Ground, Stepped-Feed and L-Slot on the Ground

The return loss results of implementation stages of designed antenna with tapered ground, stepped-feed, and L-slot on the ground between the frequencies of 1.0 and 14.0 GHz are shown in Figure 5. The impedance bandwidth performance was improved after incorporating the tapered ground, stepped-feed, and L-slot on the ground. The dimensions of each element were optimized by parametric analysis to produce UWB response with a notch band at WLAN band.

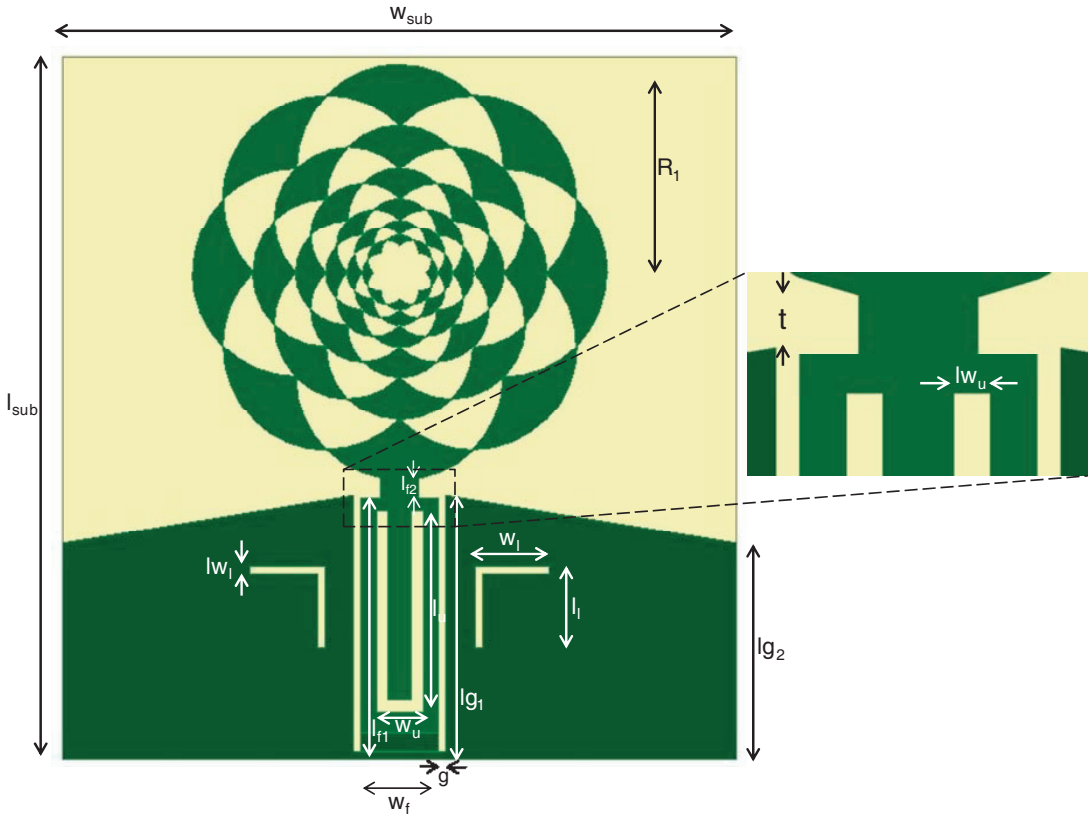

Figure 3. The structure of proposed antenna.

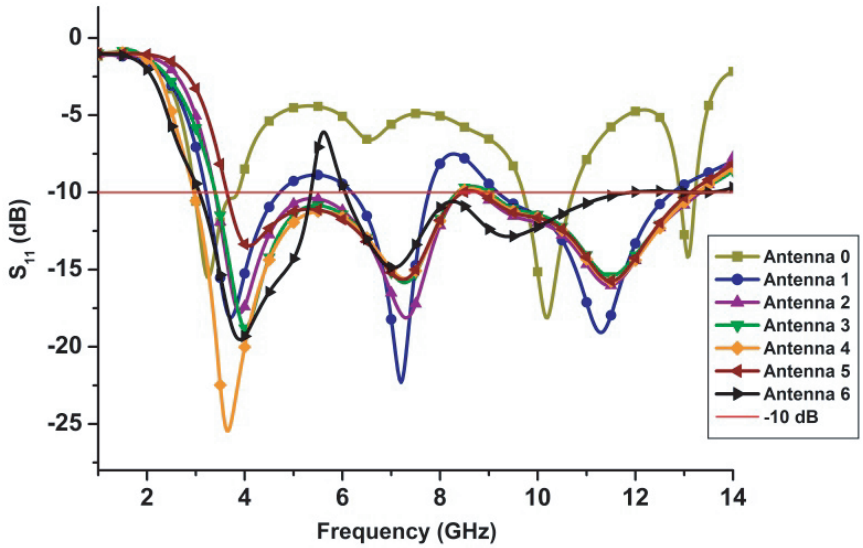

Figure 4. Return loss results of the proposed antenna with respect to its iteration.

3.3. Effect of Gap between Ground and Patch

The gap between the ground and the fractal patch acts as a matching network between the feed and antenna. The return loss results for the gap (t) distances of 0.5, 0.55, 0.6, and 0.65 mm between the frequencies of 1.0 to 15.0 GHz are shown in Figure 6. It clearly shows the impact of gap distance (t)

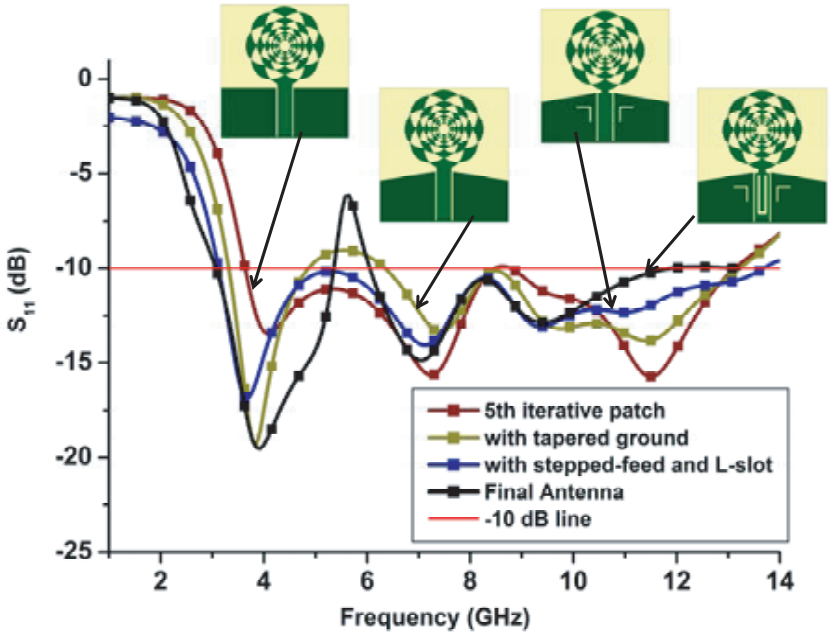

Figure 5. Return loss results of the proposed antenna when including tapered ground, stepped-feed and L-slot on the ground.

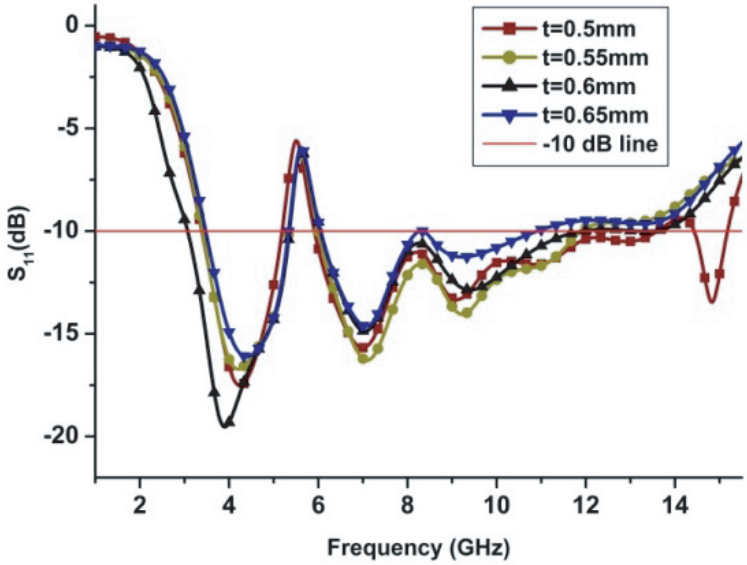

Figure 6. Return loss results of the proposed antenna for different gap between ground and patch.

between ground and patch on the impedance matching. The resonance can be varied by changing the gap (t). It is observed that at $t = 0.6$ mm, the antenna produces the better bandwidth response. By considering the ultra-wideband characteristics $t = 0.6$ mm is taken as the optimum gap between ground and patch.

3.4. Effect of Ground Plane Length l_{g2}

The trapezoid-shaped ground was designed to get good impedance matching. The ground plane outer edge length l_{g2} decides the slope range. The return loss results of l_{g2} lengths of 9.6, 9.1, and 8.6 mm

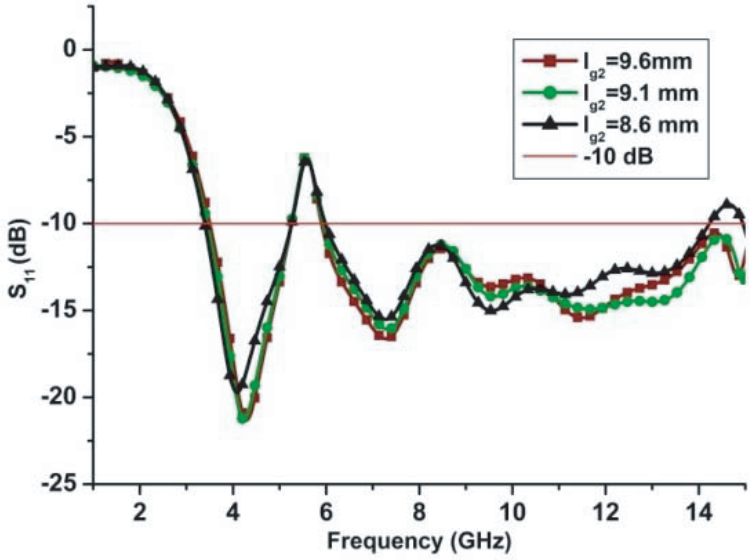

Figure 7. Return loss results of the proposed antenna for different l_{g2}.

between the frequencies of 1.0 GHz to 15.0 GHz are shown in Figure 7. It is clear from the graph that $l_{g2} = 8.6$ mm is the optimum length which produces the desired bandwidth response.

3.5. Surface Current Density

The antenna characteristics depend on how current is distributed on the surface of the antenna. The surface current density of the proposed circular fractal antenna was simulated at three different frequencies, 4.4 GHz, 7 GHz, and 9.2 GHz which are shown in Figures 8(a), (b), and (c), respectively. It is clearly seen that at 4.4 GHz, the surface current is focused on the feed, the bottom, and upper fractal elements of the radiating patch. At 7 GHz, the surface current is concentrated on the feed towards bottom fractal elements of the radiating patch. The surface current is strong on the upper portion of feed, the bottom fractal of the radiating patch at 9.2 GHz. Figure 8 illustrates that the current distribution at different places of the antenna plays an important role to produce multiple resonances.

3.6. Experimental Setup

Figure 9(a) shows the fabricated prototype of the designed circular triangle fractal antenna, and Figure 9(b) shows the pattern measurement in the anechoic chamber. The antenna was designed by using simulation and parametric study on Finite Element Method based High Frequency Structure Simulator software by Ansys corporation [23].

3.7. Frequency Domain Analysis

Figure 10 shows the simulated and measured S_{11} results of the designed circular triangle fractal antenna. It is clear that the ones. The simulated fractional bandwidth is 118.24% (8.84 GHz), and measured fractional bandwidth is 134.8 % (9.89 GHz).

The simulated and measured E-plane (x-z plane) and H-plane (x-y plane) radiation patterns of the fabricated antenna at 4.4, 7, and 9.2 GHz are shown in Figures 11(a), (b), and (c), respectively. The radiation plots illustrate that in H-plane, the nearly circular radiation pattern and in E-plane, the patterns are broadside and bidirectional, and these show practically omnidirectional pattern with a measured antenna peak gain of 11.16 dBi. A slight deviation between simulation and measurement of pattern may be due to fabrication errors, cable loss, soldering imperfections, and manual errors while measurements are carried out.

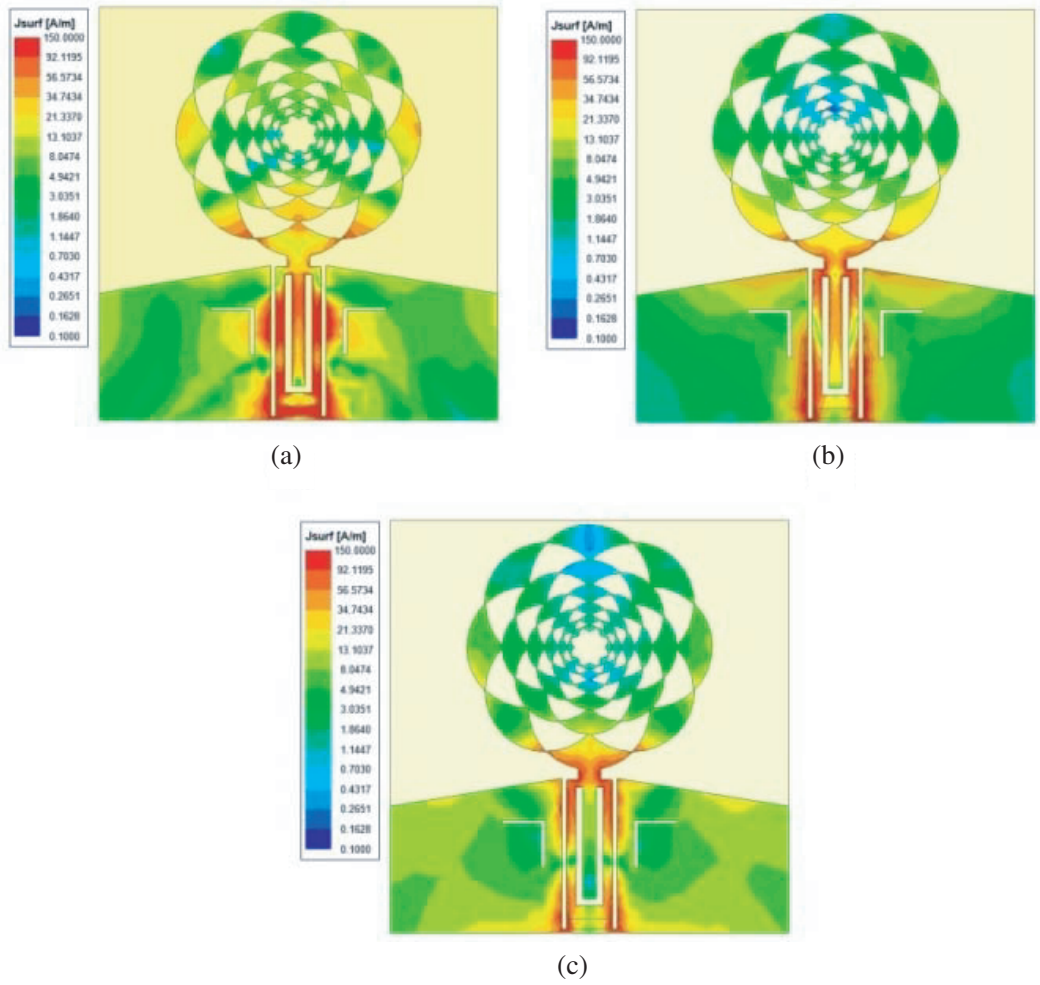

Figure 8. The simulated surface current distribution on the proposed antenna at (a) 4.4 GHz, (b) 7 GHz, (c) 9.2 GHz.

Table 2 shows the performance of various existing antenna structures compared with the proposed circular triangle fractal antenna design with respect to its shape, adopted fractal, size, bandwidth, peak gain, technique used to create rejection band, etc. The comparison is made with the existing works which utilized the fractal integration on the monopole and also made on an FR4 substrate. The proposed antenna has a wider bandwidth range of 2.39–12.28 GHz with 134.8% of fractional bandwidth which covers the entire UWB system. From Table 2, it is obvious that the proposed antenna produces better bandwidth and higher peak gain with smaller size than the compared literature.

3.8. Time Domain Analysis

Although the frequency domain results such as S_{11}, VSWR, gain, and radiation pattern were analyzed, to ensure the suggested antenna's time domain applications, it is required to carry out time domain analysis. Since the transmission happens through narrow pulses, which are prone to dispersion, the time domain analysis is very essential that can also predict the distortion of the signal radiated by the antenna. For this purpose, the group delay and fidelity factor of the proposed antenna were investigated. For these analyses, two identical antennas were kept on the two ports separated by far field distance. One antenna acts as a transmitter and another one as a receiver. The pair of antennas were arranged in two different configurations, i.e., face-to-face and side-by-side, for characterizing the time domain results.

(a) (b)

Figure 9. (a) Fabricated prototype of the proposed antenna. (b) Pattern measurement in an anechoic chamber.

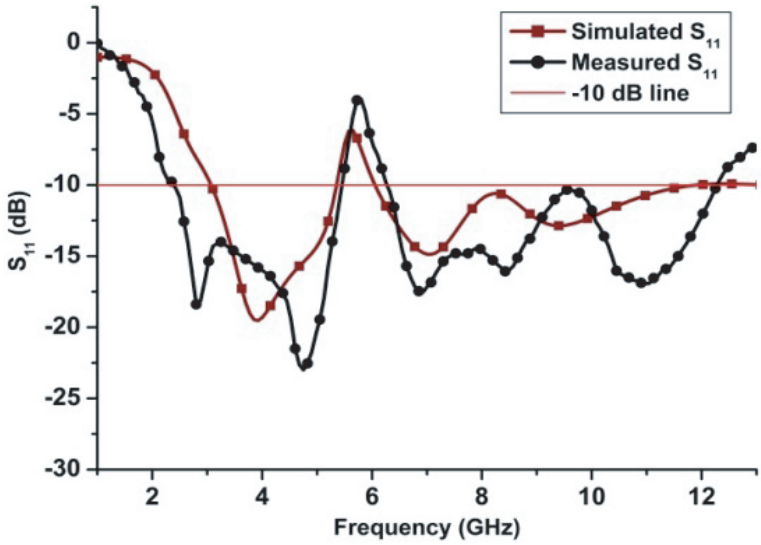

Figure 10. Simulated and measured return loss results of the proposed circular triangle fractal antenna.

3.9. Group Delay of Antenna

The group delay is an essential metric for UWB system. It shows the amount of pulse distortion and far-field phase linearity. The group delay $\tau_g(\omega)$ is defined as the negative rate of change of phase with respect to frequency. This can be expressed as (6)

$$\tau_g(\omega) = \frac{-d\varphi(f)}{2\pi df} \tag{6}$$

where '$\varphi(f)$' is the frequency-dependent phase, and 'f' is the frequency of the excited input signal. Figure 12 shows the group delay characteristics of the proposed circular triangle fractal antenna. From the figure, it is clear that the group delay of the antenna ranges below 1 ns. For desired time domain response, the group delay should be constant throughout the UWB. In this aspect too, the proposed antenna's performance is reinstated through the group delay plot.

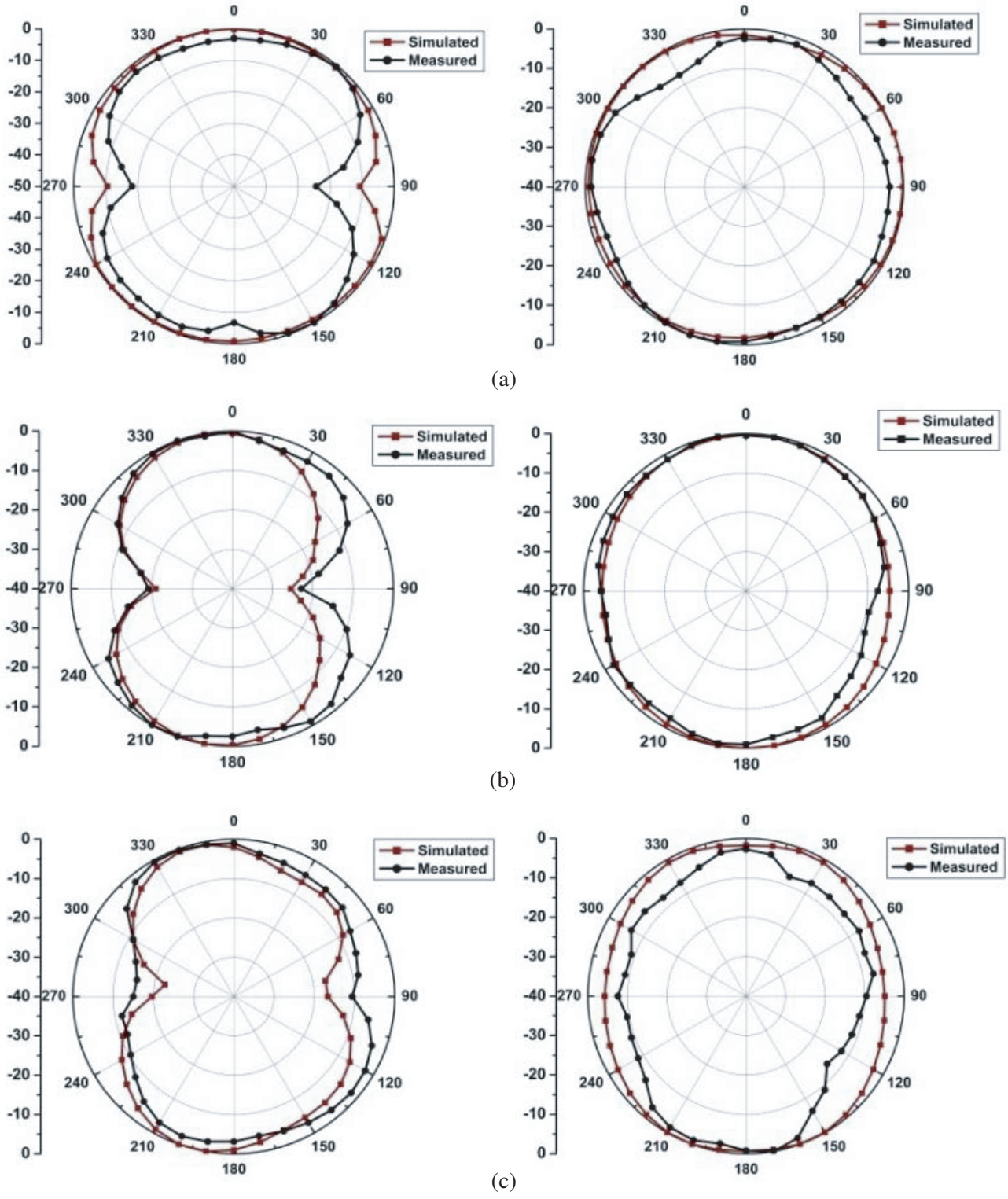

Figure 11. (a) Simulated and measured E-plane and H-plane radiation patterns at 4.4 GHz. (b) Simulated and measured E-plane and H-plane radiation patterns at 7 GHz. (c) Simulated and measured E-plane and H-plane radiation patterns at 9.2 GHz.

Table 2. Performance comparison.

Ref. No.	Fractal structures adopted	Size (mm^2)	Operating Band (GHz)	Band of rejection	Peak Gain (dBi)	Notching Technique
[15]	Sierpinski carpet fractal with circular monopole	40×38	3–12	5.15–5.825 GHz; IEEE802.11a & HIPERLAN/2	6	Meandered slot on the radiating patch
[16]	Hexagonal Sierpinski carpet fractal	33×32	3–12	5.15–5.825 GHz; IEEE802.11a & HIPERLAN/2	6	'Y' slot on the feed line that extends to radiating patch
[17]	Circular shaped Apollonian fractal	44×58	1.8–10.6	5.125–5.825 GHz; IEEE 802.11a, HIPERLAN/2	6	A couple of L-shaped slots on the ground
[18]	Modified Sierpinski square fractal antenna	34×34	3.1–10.6	5–6 GHz; WLAN	5	$\cap$-slot on the feed line
[19]	Modified circular split ring fractal structure	26×27	2.19–13.95	4.67–6.21 GHz; WLAN	5	A sectorial-circular slot in the patch
[20]	Wheel shaped modified fractal antenna	32×36	2.93–9.53	NA	5.17	NA
[21]	Sierpinski square fractal slot on decagonal shaped monopole	28×28	3.50–15.1	NA	5.95	NA
Proposed	Circular triangle fractal shaped monopole	28×27	2.39–12.28	5.45–6.27 GHz; WLAN	11.16	U shaped slot on the feed

3.10. Fidelity Factor of an Antenna

The fidelity factor needs to be computed to validate the correlation between the transmitted and received signals. The default Gaussian pulse provided in the HFSS Software which has spectrum spanning from 3.1 to 10.6 GHz was used as the input signal. The face-to-face and side-by-side orientations are examined between two identical antennas which act as a transceiver separated by 300 mm distance. Figure 13 shows the setup for fidelity analysis. The fidelity factor is the peak magnitude of the cross correlation between the excited input pulse and received output pulse. This was calculated in MATLAB for the signals obtained from the setup by using Equation (7).

$$FF = \max_{\tau} \left[\frac{\int_{-\infty}^{+\infty} s_t(t) s_r(t-\tau) dt}{\sqrt{\int_{-\infty}^{+\infty} s_t^2(t)\, dt \int_{-\infty}^{+\infty} s_r^2(t)\, dt}} \right] \tag{7}$$

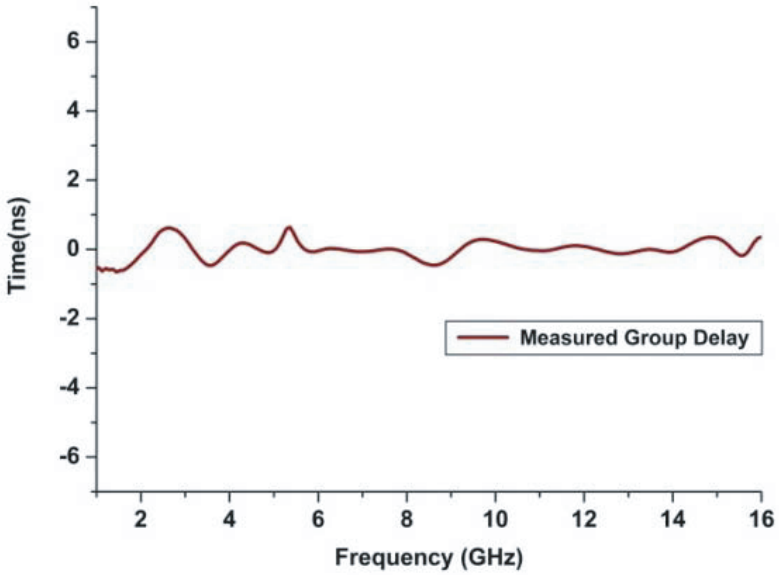

Figure 12. Measured Group Delay response of the proposed antenna.

where $s_t(t)$ and $s_r(t)$ are the excited input pulse and received output pulse, respectively. τ is the amount of time shift. Figure 13 shows the excited input pulse and received output pulse of the proposed circular triangle fractal antenna which depicts the proposed antenna's performance in both the cases. It is clear from the figure that the face-to-face configuration produces the signal with less distortion than side-by-side configuration. The fidelity factors for the face-to-face configuration and side-by-side configuration are 0.83 and 0.73, respectively. From the observation, it is clearly seen that the received output pulse maintains the excited input pulse shape.

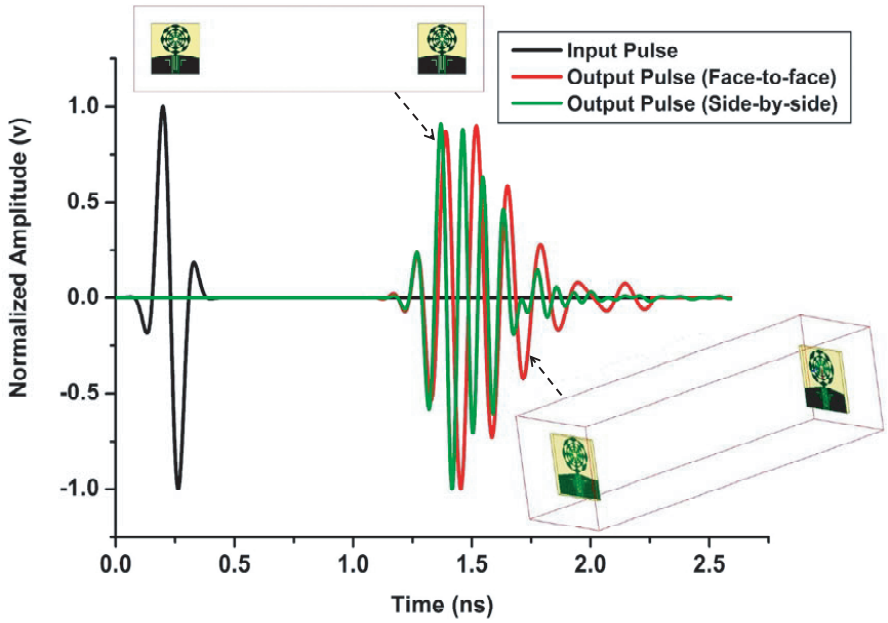

Figure 13. Excited input pulse and received output pulses with Face-to face and Side-by-side configuration.

4. CONCLUSION

This paper has presented the simulated and experimental results of a circular triangle fractal antenna for high gain UWB communications with band rejection capability. From results, it is clear that the proposed circular triangle fractal antenna is ideal for the high gain UWB communication systems. The optimization has been done for various dimensional parameters to achieve the required characteristics. The experimental outcomes revealed good concurrence with the simulated results in the obtained impedance bandwidth of 9.89 GHz from 2.39 to 12.28 GHz which corresponds to wide bandwidth of over 134.8%. The fidelity factors for the face-to-face and side-by-side configurations are 0.83 and 0.73, respectively, and group delay varies within 1 ns. It is found that the antenna exhibits a good response in both the frequency and time domains. The peak gain detected is 11.16 dBi. In addition to compactness and high gain, the antenna gives stable far-field radiation performance in the desired UWB range, which makes the proposed circular triangle fractal antenna useful for UWB applications.

REFERENCES

1. FCC report and order, revision of part 15 of the commission's rules regarding ultra-wideband transmission systems. FCC02-48, 2002.
2. Oppermann, I., M. Hämäläinen, J. Iinatti (eds.), *UWB: Theory and Applications*, John Wiley & Sons, 2004.
3. Karmakar, A., S. Verma, M. Pal, and R. Ghatak, "An ultra-wideband monopole antenna with multiple fractal slots with dual band rejection characteristics," *Prog. Electromagn. Res. C*, Vol. 31, 185–197, 2012.
4. Rani, B. R. and S. K. Pandey, "A parasitic hexagonal patch antenna surrounded by same shaped slot for WLAN, UWB applications with notch at vanet frequency band," *Microw. Opt. Technol. Lett.*, Vol. 58, No. 12, 2996–3000, 2016.
5. Parchin, N. O., H. J. Basherlou, and R. A. Abd-Alhameed, "UWB microstrip-fed slot antenna with improved bandwidth and dual notched bands using protruded parasitic strips," *Prog. Electromagn. Res. C*, Vol. 101, 261–273, 2020.
6. Ryu, K. S. and A. A. Kishk, "UWB antenna with single or dual band-notches for lower WLAN band and upper WLAN band," *IEEE Trans. Antennas Propag.*, Vol. 57, No. 12, 3942–3950, 2009.
7. Fertas, K., F. Ghanem, A. Azrar, and R. Aksas, "UWB antenna with sweeping dual notch based on metamaterial SRR fictive rotation," *Microw. Opt. Technol. Lett.*, Vol. 62, No. 2, 956–963, 2020.
8. Sanmugasundaram, R., N. Somasundaram, and R. Rajkumar, "Ultrawideband notch antenna with EBG structures for WiMAX and satellite application," *Prog. Electromagn. Res.*, Vol. 91, 25–32, 2020.
9. Mandelbrot, B. B., *Fractals. Form, Chance and Dimension*, Freeman, 1977.
10. Cohen, N., "Fractal antenna applications in wireless telecommunications," *Professional Program Proceedings. Electronic Industries Forum of New England*, 43–49, 1997.
11. Werner, D. H. and S. Ganguly, "An overview of fractal antenna engineering research," *IEEE Antennas Propag Mag.*, Vol. 45, No. 1, 38–57, Mar. 2003.
12. Haji-hashemi, M. R., M. Moradian, and H. Mirmohammad-Sadeghi, "Space-filling patch antennas with CPW feed," *Prog. Electromagn. Res. S.*, Vol. 2, No. 1, 69–73, 2006.
13. Ramya, M. C. and B. R. Rani, "A compendious review on fractal antenna geometries in wireless communication," *International Conference on Inventive Computation Technologies (ICICT), IEEE*, 888–893, 2020.
14. Ramya, M. C., and B. R. Rani, "Fractal based ultra-wideband antenna design: A review," *Planar Antennas: Design and Applications*, P. K. Malik (ed.), 1st Edition, CRC press, 131–151, 2021.
15. Ghatak, R., A. Karmakar, and D. R. Poddar, "A circular shaped Sierpinski carpet fractal UWB monopole antenna with band rejection capability," *Prog. Electromagn. Res.*, Vol. 24, 221–234, 2011.

16. Ghatak, R., A. Karmakar, and D. R. Poddar, "Hexagonal boundary Sierpinski carpet fractal shaped compact ultrawideband antenna with band rejection functionality," *AEU - Int. J. Electron. Commun.*, Vol. 67, No. 3, 250–255, 2013.
17. Ghatak, R., B. Biswas, A. Karmakar, and D. Poddar, "A circular fractal UWB antenna based on Descartes circle theorem with band rejection capability," *Prog. Electromagn. Res. C*, Vol. 37, 235–248, 2013.
18. Choukiker, Y. K. and S. K. Behera, "Modified Sierpinski square fractal antenna covering ultra-wide band application with band notch characteristics," *IET Microw. Antennas Propag.*, Vol. 8, No. 7, 506–512, 2014.
19. Garg. R. K., M. V. Nair, S. Singhal, and R. Tomar, "A new type of compact ultra-wideband planar fractal antenna with WLAN band rejection," *Microw. Opt. Technol. Lett.*, Vol. 62, No. 7, 2537–2545, 2020.
20. Gupta, M. and V. Mathur, "Wheel shaped modified fractal antenna realization for wireless communications," *AEU - Int. J. Electron. Commun.*, Vol. 79, 257–266, 2017.
21. Ali, T., B. K. Subhash, and R. C. Biradar, "A miniaturized decagonal Sierpinski UWB fractal antenna," *Prog. Electromagn. Res. C*, Vol. 84, 161–174, 2018.
22. Balanis, C. A., *Antenna Theory: Analysis and Design*, 4th Edition, John Wiley & Sons, 2016.
23. Ansoft Corp., HFSS, ver. 14.0, Pittsburgh, PA, USA [Online]. Available: http://www.ansys.com.